Published in final edited form as:
Ophthalmology. 2013 September ; 120(9): 1901–1908. doi:10.1016/j.ophtha.2013.01.066.

Analysis of Choroidal Morphology and Vasculature in Healthy Eyes Using Spectral-Domain Optical Coherence Tomography

Lauren A Branchini, BA[1,**], **Mehreen Adhi, MBBS**[1,**], **Caio V Regatieri, MD, PhD**[1], **Namrata Nandakumar, MD**[1], **Jonathan J Liu, MS**[2], **Nora Laver, MD**[1], **James G Fujimoto, PhD**[2], and **Jay S Duker, MD**[1]

[1]New England Eye Center, Tufts Medical Center, Boston, Massachusetts

[2]Dept of Electrical Engineering and Computer Science, Research Laboratory of Electronics, Massachusetts Institute of Technology, Cambridge, Massachusetts

Abstract

Objective—To analyze the morphology and vasculature of the choroid in healthy eyes using spectral-domain optical coherence tomography (SD-OCT).

Design—Cross-sectional retrospective review.

Participants—Forty-two healthy subjects (42 eyes), with no ocular disease who underwent high-definition scanning with Cirrus HD-OCT at the New England Eye Center, Boston, Massachusetts between November 2009 and September 2010.

Methods—The SD-OCT images were evaluated for morphological features of the choroid, including the shape of the choroid-scleral border, location of the thickest point of choroid and regions of focal choroidal thinning. Total choroidal thickness and large choroidal vessel layer thickness were measured by two independent observers experienced in analyzing OCT images using the Cirrus linear measurement tool at the fovea, 750μm nasal and temporal to the fovea. Custom software was used to calculate the ratio of choroidal stroma to the choroidal vessel lumen.

Main Outcome Measures—Qualitative assessment of the choroidal morphology, quantitative analysis of choroidal vasculature and use of a novel automated software to determine the ratio of choroidal stromal area to the area of choroidal vessel lumen.

Results—The 42 subjects had a mean age of 51.6 years. All subjects (100%) had a “bowl” or convex shape to the choroid-sclera junction and the thickest point of the choroid was under the fovea in 88.0% of the subjects. The mean choroidal thickness was 256.8±75.8μm, thickness of the large choroidal vessel layer was 204.3±65.9μm and that of medium choroidal vessel layer/ choriocapillaris layer was 52.9±20.6μm beneath the fovea. The ratio of large choroidal vessel layer thickness to the total choroidal thickness beneath the fovea was 0.7±0.06. The software

Corresponding Author/Reprint Requests: Jay S. Duker, MD, New England Eye Center, 800 Washington Street, Boston, MA 02111, Phone: 617-636-4677, Fax: 617-636-4866, Jduker@tuftsmedicalcenter.org.
**The first and second authors contributed equally to this study

Conflict of Interest

James G. Fujimoto, receives royalties from intellectual property owned by M.I.T. and licensed to Carl Zeiss Meditech, Inc.; O, has stock options in Optovue, Inc.

Jay S. Duker, receives research support from Carl ZeissMeditech, Inc. and Optovue, Inc.

generated ratio of choroidal stromal area to the choroidal vessel lumen area to be 0.27±0.08, suggesting that choroidal vessel lumen forms a greater proportion of the choroid than choroidal stroma in healthy eyes.

Conclusions—This is the first study describing the morphology and vasculature of choroid in healthy eyes from 1-line raster scans obtained using SD-OCT. The method described holds promise, and has immediate clinical utility in recognizing subtle changes in choroidal morphology and the role of choroidal angiopathy in various disease states, that in the future might inform new treatment modalities.

The term choroid is derived from the Greek words for “membrane” and “form”. It is a vascularized and pigmented tissue that extends from the ora serrata anteriorly to the optic nerve posteriorly. Histological investigations of the choroid demonstrate that it is 0.22 mm thick posteriorly and 0.10–0.15 mm thick anteriorly, and is comprised of three main vascular layers: the choriocapillaris, Sattler’s layer and Haller’s layer. (Figure 1). [1]

The choroid is responsible for vascular support of the outer retina. A structurally and functionally normal choroidal vasculature is essential for retinal function: abnormal choroidal blood volume and/or compromised flow can result in photoreceptor dysfunction and death.[2] Consequently, the choroid plays a vital role in the pathophysiology of many conditions such as age-related macular degeneration (AMD), central serous chorioretinopathy and diabetic retinopathy.[3–5]

Probing structural and functional parameters of the choroid is important for understanding of disease progression. Techniques that are currently used to clinically assess the choroidal vasculature in vivo include fluorescein angiography (FA) and indocyanine green angiography (ICG).[6] However, angiography is not quantitative, does not provide three-dimensional anatomic information about the retinal pigment epithelium (RPE) or the choroidal layers, and is not without risk.[7]

By contrast, optical coherence tomography (OCT) is a non-invasive imaging modality that uses low coherence reflectometry to obtain cross sectional images of the retina on a micron scale [8]. The recently developed spectral-domain OCT (SD-OCT) systems, dramatically increase image acquisition speed and resolution, thereby improving scan quality.[9] Recent reports demonstrate successful measurement of choroidal thickness in normal and pathologic states using SD-OCT devices.[10–15] To the best of our knowledge however, no description of the morphological characteristics of the healthy choroid using SD-OCT has been undertaken to date. We have observed that there are differences in the structure of the choroid on SD-OCT in disease states such as AMD and other retinal diseases, which are not adequately described by measuring sub-foveal choroidal thickness alone (Figure 2). This study was designed to analyze the morphology of the choroid and also the assessment of its vasculature manually as well as with a custom software, using high definition 1-line raster scans obtained using SD-OCT. These methods may be useful in differentiating healthy choroid from choroid affected by pathology in future.

METHODS

Subjects

A retrospective analysis was performed on 42 eyes of 42 healthy subjects, who underwent high-definition 1-line raster scanning at the New England Eye Center, Tufts Medical Center, Boston, Massachusetts between November 2009 and September 2010. None of the eyes had any previous or concurrent retinal or choroidal pathology. Subjects with myopic refractive error of greater than 6.0 diopters were excluded with the understanding that pathological myopia may have a significant effect on the detailed analysis of the choroid. All subjects

had a best-corrected visual acuity of 20/20 or greater and underwent fundus examination. This study was approved by the institutional review board of Tufts Medical Center and is adherent to the tenets of the Declaration of Helsinki.

SD-OCT Scanning

SD-OCT scanning was performed using Cirrus high definition (HD) (Carl Zeiss Meditec Inc., Cublin, California, USA), which operates at a wavelength of 840μm. The scan pattern employed was the 1-line raster, which is a 6-mm line consisting of 4096 A-scans, an imaging speed of 27,000 A-scans per second, an axial resolution of 5μm a transverse resolution of 15μm in tissue and averages 20 frames (B-scans). Averaging of imaging results in reduced "speckle," which enhances the continuity and sharpens the tissue features. Image averaging typically increases signal-to-noise ratio (SNR) in proportion to the square root of the number of images averaged. The images were taken in the usual manner, and were not inverted to bring the choroid closer to the zero-delay line, as inversion of images using Cirrus results in low-resolution and a pixilated image due to signal processing artifacts. Enhanced depth imaging (EDI) which automatically sets the choroid closer to the zero delay line, and thus theoretically provides a better visualization of the choroid-scleral interface, was not available at the time the images were obtained. All scans had an intensity of 6/10 or greater and were taken as close to the fovea as possible, so as to image the thinnest part of the macula. This was done to avoid slight differences in positioning, so that the analysis of the morphological features and vasculature of the choroid can be done precisely. One eye per patient was selected for analysis. If scans from both eyes met the inclusion criteria, then the scan from the eye in which the choroid-sclera border could be most clearly visualized was selected. Of the 42 eyes, 18 right eyes and 24 left eyes were analyzed.

Morphological Description of the Choroid

Two independent raters experienced in examining SD-OCT images evaluated the choroid for morphological features. A third rater was consulted when the two raters disagreed, and majority determination was used for the purpose of analysis. The clarity of the choroid-sclera junction was examined. The contour and shape of the choroid-scleral junction was also evaluated as being either a smooth "bowl" or convex shape vs. having more than one inflection point or an "S" or an irregular shape. Whether or not the thickest point of the choroid was sub-foveal, as well as if there was any focal thinning of the choroid was also observed. The continuum in size of choroidal vessels axially was also observed with "even" meaning that larger vessels lie closer to the choroid-sclera junction and smaller vessels closer to the Bruch's membrane/RPE and "uneven" meaning the presence of large vessels adjacent to the Bruch's membrane/RPE. Distribution of large vessels in the nasal-temporal plane was also evaluated as either being evenly spaced or not evenly spaced. Intensity of the choroidal stroma between the large vessels and the penetration of scleral vessels into the choroid-scleral border were also evaluated.

Analysis of Choroidal Vasculature

The luminal diameter of large choroidal vessels (including arteries and veins) in healthy eyes ranges from 28.2 ± 11.2μm to 37.1 ± 12.5μm on histology.[16] Histological analysis may cause alteration of the tissue due to postmortem changes and processing artifacts,[16] which makes comparison of the of the thickness of the choroidal vascular layers on OCT and on histology impractical and erroneous. A pilot study performed by our group involved identification of the smallest visible large vessel layer located in close proximity to the choroid-sclera border on SD-OCT images of 42 healthy subjects (42 eyes) at any location on the 6mm 1-line raster SD-OCT scan. This was then measured in the nasal-temporal plane using the Cirrus linear measurement tool, by two independent raters, and their average was

calculated. While the differences in the transverse and axial resolutions of the SD-OCT system may affect the accuracy of measurements, however, we obtained the diameters of vessels only in the nasal-temporal plane (transverse plane). Raters experienced in analyzing OCT images performed this pilot. The mean diameter of the smallest large choroidal vessels measured on the SD-OCT images of healthy eyes was 100μm (range: 86μm–108μm) (unpublished data). This was used as a cut-off for defining a large choroidal vessel for the choroidal vasculature analysis on SD-OCT in the present study.

For choroidal vasculature analysis, the choroidal thickness was measured by two independent observers perpendicularly from the outer edge of the hyper-reflective RPE to the inner sclera at three locations; at the fovea, 750μm temporal to the fovea, and 750μm nasal to the fovea. At the same locations, large choroidal vessels measuring ≥100 μm, located close to the choroid-scleral border and within the closest proximity to the locations of the choroidal thickness measurement lines were identified. Perpendicular lines from the inner most point of the large choroidal vessels were drawn at the same locations, which intersected the choroidal thickness measurement lines. Following this, the thickness of the large choroidal vessel layer (Haller's layer) was measured perpendicularly from the inner border of the sclera to the intersection point on the choroidal thickness measurement lines at all locations (Figure 3). The measurements of the large choroidal vessel layer were subtracted from the total choroidal thickness at all locations, to obtain the distance of the large choroidal vessel layer to Bruch's membrane/RPE complex, which corresponds to the choriocapillaris layer and the Sattler's layer (medium choroidal vessel layer) thickness. These two layers were analyzed together (as a complex), since the current OCT technology does not allow for delineation of these layers separately. The ratio of the thickness of the large choroidal vessel layer to the total choroidal thickness was also calculated. Two independent raters experienced in analyzing OCT images performed all the measurements and the average measurements were used for the purpose of analysis.

Light/Dark Ratio

Custom software was developed using MATLAB (Natick, MA: The Math Works Inc.). A region of interest (ROI) of 1.5mm width, centered below the fovea in the choroid was manually selected. The light/dark ratio was calculated according to the threshold level obtained by Otsu's method, which minimizes the intra-class variance of the threshold of the black and white pixels. For example, a light/dark ratio greater than 1 indicates that there are more bright pixels than dark pixels in the selected ROI. The light pixels correspond to the area of choroidal stroma found within the ROI, while the dark pixels correspond to choroidal vessel lumen area within the ROI (Figure 4).

Statistical Analysis

All data was expressed as mean ± standard deviation (SD). Pearson correlation was used to assess the inter-observer correlation of all the measurements of the choroidal vasculature. All descriptive statistics and inter-observer correlations were performed using Graph Pad Prism 5.0 software for Macintosh (GraphPad Software, La Jolla, CA).

RESULTS

The 42 subjects had a mean age of 51.6 ± 21.02 years (range: 23–89 years). A summary of the morphological features of the choroid is shown in Table 1. All qualitative observations had a strong inter-observer correlation.

Analysis of Choroidal Vasculature

The total choroidal thickness, thickness of the large choroidal vessel layer (Haller's layer), distance of the large choroidal vessel layer to Bruch's membrane/RPE complex, which corresponds to the choriocapillaris layer and the Sattler's layer (medium choroidal vessel layer) thickness and the mean ratio of the thickness of the large choroidal vessel layer to the total choroidal thickness at the fovea, 750μm temporal to the fovea and 750μm nasal to the fovea are summarized in Table 2. All measurements had a strong inter observer correlation (Table 2).

Light/Dark Ratio

Custom software (described above) generated a mean light-dark ratio of 0.27 ± 0.08. This number can be interpreted to mean that the choroid of a healthy eye has, on average, a higher proportion of choroidal vessel lumen (dark pixels) than choroidal stroma (bright pixels) in a sub-foveal cross-sectional ROI.

DISCUSSION

This study demonstrates an assessment of various morphological features of a healthy choroid and analysis of the vascular layers of the choroid using SD-OCT. In addition, this study presents the utility of custom software to assess the ratio of choroidal stroma to the choroidal vascular lumen in healthy eyes, a method that can be used clinically for the quantitative assessment of the choroidal vessel density. Because a precise clinical understanding of choroidal changes might be important for an accurate assessment of many diseases, the choroid has been evaluated by ICG[6,17] and laser doppler flowmetry,[18,19] which analyze the blood flow in the choroidal vessels. Although these techniques are useful for determining vessel abnormalities or changes in the choroidal blood flow, they do not provide any three-dimensional anatomic information of the choroidal vascular layers. Recent studies have demonstrated successful measurement of the choroidal thickness in normal and pathological states, such as age-related macular degeneration, central serous chorioretinopathy, high myopia and diabetic retinopathy.[10–15,20] In addition to observing changes in choroidal thickness, our group has observed distortion in the morphology of the choroid in a number of pathological conditions. To the best of our knowledge, this is the first study describing the morphological features of the choroid other than the total choroidal thickness using standard clinically available SD-OCT, and describes novel custom software for the analysis of the large choroidal vessel density. Recent studies have attempted to describe the thickness of the vascular layers of the choroid[21] and measurement of the choroidal vessel density[22] using C-scans generated from post acquisition processing of the images obtained using SD-OCT. However, using C-scans for the assessment of choroidal vascular layers as described by Zhang et al[21], requires complex processing of images post acquisition, which may have limitations for immediate clinical utility. In addition, while choriocapillaris were delineated separately, the medium choroidal vascular layer and the large choroidal vascular layers were assessed together as the "choroidal vasculature" in that study.[21] The present study describes the analysis of choroidal vasculature in healthy eyes using 1-line raster B scans obtained using SD-OCT, which are currently rampantly used in the ophthalmic practice. This and the methods for analysis of the choroidal morphology and choroidal vessel density may have immediate clinical applications to help differentiate between healthy and diseased states.

This study shows that the choroid is thickest sub-foveally and thins out much more nasally than temporally in healthy eyes. These findings agree with previous reports.[23,24] The choroid is convex or "bowl" shaped (as seen on histology, Figure 1), and there is no focal thinning of the choroid in healthy eyes. In addition, the continuum of choroidal vessels is

"even" (as seen on histology, Figure 1), the large choroidal vessels are "evenly spaced" and the choroid-scleral border is clearly identifiable in more than 90% of the healthy eyes. These findings may provide a benchmark for the assessment of morphologic changes involving the choroid in various pathologic states, which could potentially provide a better understanding of choroidal angiopathy in retinal diseases.

Figure 1 demonstrates a histological image of a healthy eye. The three choroidal vascular layers can be identified. Histological fixation produces artifacts including shrinkage which further make a systematic correlative investigation of choroidal choroidal vasculature on OCT vs. histology impractical.[25] Thus, this study refrained from making any conclusive quantitative comparisons between SD-OCT images and histology. Since Cirrus HD-OCT has an axial resolution of 5μm in tissue, it is difficult to distinguish between the choriocapillaris and medium choroidal vessel layer (Sattler's layer). For this reason, this study analyzed the thickness of these layers as a complex, which along with the thickness of the large choroidal vessel layer, was achieved in this study with a strong inter-observer correlation. This investigation found the thickness of the mean sub-foveal large choroidal vessel layer thickness to be 204.3±65.9μm, that of the mean sub-foveal medium choroidal vessel layer/choriocapillaris layer to be 52.86μm±20.63μm, and the mean ratio of the large choroidal vessel layer to the total choroidal thickness of 0.7±0.06. There was no significant variability of the Haller's layer thickness amongst the three studied locations. Furthermore, this study quantified through automated software techniques, the ratio of the region of sub-foveal choroidal vessel lumen to that of the region of choroidal stroma, that is, the density of the choroidal vessels, showing that in-vivo assessment of choroidal vasculature using SD-OCT shows a greater proportion of choroidal vessel lumen than choroidal stroma beneath the fovea in healthy eyes. This was expected in a healthy choroid because the choroid is a vascular tissue. The mean vessel density described by Sohrab et al in the outer part of the choroid in healthy eyes is ~87% (79–93%).[22] This analysis and determination of the vessel to stroma ratio in the different layers of the choroid may be helpful in determining choroidal vascular changes in vascular diseases such as diabetic retinopathy and age-related macular degeneration, which present with vascular atrophy and increase in extracellular matrix deposition. While it is difficult to ascertain what an abnormal light/dark ratio is until studies comparing the healthy to diseased eyes are performed, a ratio greater than 1 suggests a greater proportion of the choroidal stroma to choroidal vessels, which is theoretically abnormal, as choroid is a vascular tissue. None of the healthy subjects in the present study had a light/dark ratio greater than 1. In addition, the intensity of the choroidal stroma did not vary in the healthy eyes to determine the relationship between the light/dark ratio and the intensity of the choroidal stroma. This may be important to assess in diseases such as age-related macular degeneration and diabetic retinopathy.

Future techniques for visualization of the choroid by OCT include using a wavelength centered near 1050nm, which has been shown to have increased penetration, making the visualization of the choroid-scleral border with greater precision.[26,27] Another promising technology, Doppler OCT, is able to evaluate blood flow and volume.[28–30] Wang et. al described decreased blood flow and arterial velocity in patients with glaucoma, nonarteritic ischemic optic neuropathy and proliferative diabetic retinopathy compared to healthy subjects using Doppler OCT.[31] The use of en-face imaging, which allows for visualization of three dimensional OCT data in a fundus projection (C-scans), may be important in the future for evaluation the vascular layers of the choroid.[21,22,32] These technologies may further enhance our understanding of the choroidal vasculature, and could potentially also help resolve the medium choroidal vessel layer and the choriocapillaris layer separately. In addition, using C-scans, it is plausible to ascertain the variability of the thickness of the choroidal vascular layers[21,22]. The present study is limited in describing the thickness of the vascular layers of the choroid only within a small region beneath the fovea.

In conclusion, this study describes the morphology and vasculature of the choroid in healthy eyes with a detailed methods using SD-OCT. These method hold promise in recognizing new subtle changes in choroidal morphology, in particular the role of choroidal angiopathy in various disease states, that in the future might inform new treatment modalities. Further studies looking at the morphology and vasculature of the choroid in diseased states are underway.

Acknowledgments

Financial Support

This work was supported in part by a Research to Prevent Blindness Challenge grant to the New England Eye Center/Department of Ophthalmology -Tufts University School of Medicine, NIH contracts RO1-EY11289-25, R01-EY13178-10, R01-EY013516-07, R01-EY019029-02, Air Force Office of Scientific Research FA9550-10-1-0551 and FA9550-10-1-0063.

References

1. Guyer, DR.; Schachat, AP.; Green, WR. The choroid: structural considerations. In: Ryan, SJ., editor. Retina. 4. Vol. 1. Philadelphia, PA: Elsevier Mosby; 2006. p. 33-4.
2. Hidayat AA, Fine BS. Diabetic choroidopathy. Light and electron microscopic observations of seven cases. Ophthalmology. 1985; 92:512–22. [PubMed: 2582331]
3. Bressler NM. Antiangiogenic approaches to age-related macular degeneration today. Ophthalmology. 2009; 116(suppl):S15–23. [PubMed: 19800535]
4. Cao J, McLeod S, Merges CA, Lutty GA. Choriocapillaris degeneration and related pathologic changes in human diabetic eyes. Arch Ophthalmol. 1998; 116:589–97. [PubMed: 9596494]
5. Gemenetzi M, De Salvo G, Lotery AJ. Central serous chorioretinopathy: an update on pathogenesis and treatment. Eye (Lond). 2010; 24:1743–56. [PubMed: 20930852]
6. Spaide RF, Yannuzzi LA, Slakter JS, et al. Indocyanine green videoangiography of idiopathic polypoidal choroidal vasculopathy. Retina. 1995; 15:100–10. [PubMed: 7542796]
7. Yannuzzi LA, Rohrer KT, Tindel LJ, et al. Fluorescein angiography complication survey. Ophthalmology. 1986; 93:611–7. [PubMed: 3523356]
8. Huang D, Swanson EA, Lin CP, et al. Optical coherence tomography. Science. 1991; 254:1178–81. [PubMed: 1957169]
9. Wojtkowski M, Leitgeb R, Kowalczyk A, et al. In vivo human retinal imaging by Fourier domain optical coherence tomography. J Biomed Opt. 2002; 7:457–63. [PubMed: 12175297]
10. Chung SE, Kang SW, Lee JH, Kim YT. Choroidal thickness in polypoidal choroidal vasculopathy and exudative age-related macular degeneration. Ophthalmology. 2011; 118:840–5. [PubMed: 21211846]
11. Fujiwara T, Imamura Y, Margolis R, et al. Enhanced depth imaging optical coherence tomography of the choroid in highly myopic eyes. Am J Ophthalmol. 2009; 148:445–50. [PubMed: 19541286]
12. Imamura Y, Fujiwara T, Margolis R, Spaide RF. Enhanced depth imaging optical coherence tomography of the choroid in central serous chorioretinopathy. Retina. 2009; 29:1469–73. [PubMed: 19898183]
13. Maruko I, Iida T, Sugano Y, et al. Subfoveal choroidal thickness after treatment of central serous chorioretinopathy. Ophthalmology. 2010; 117:1792–9. [PubMed: 20472289]
14. Maruko I, Iida T, Sugano Y, et al. Subfoveal choroidal thickness after treatment of Vogt-Koyanagi-Harada disease. Retina. 2011; 31:510–7. [PubMed: 20948460]
15. Regatieri CV, Branchini L, Carmody J, et al. Choroidal thickness in patients with diabetic retinopathy analyzed by spectral-domain optical coherence tomography. Retina. 2012; 32:563–8. [PubMed: 22374157]
16. Spraul CW, Lang GE, Lang GK, Grossniklaus HE. Morphometric changes of the choriocapillaris and the choroidal vasculature in eyes with advanced glaucomatous changes. Vision Res. 2002; 42:923–32. [PubMed: 11927356]

17. Scheider A, Nasemann JE, Lund OE. Fluorescein and indocyanine green angiographies of central serous choroidopathy by scanning laser ophthalmoscopy. Am J Ophthalmol. 1993; 115:50–6. [PubMed: 8420378]

18. Tamaki Y, Araie M, Kawamoto E, et al. Non-contact, two-dimensional measurement of tissue circulation in choroid and optic nerve head using laser speckle phenomenon. Exp Eye Res. 1995; 60:373–83. [PubMed: 7789417]

19. Grunwald JE, Hariprasad SM, DuPont J, et al. Foveolar choroidal blood flow in age-related macular degeneration. Invest Ophthalmol Vis Sci. 1998; 39:385–90. [PubMed: 9477998]

20. Koizumi H, Yamagishi T, Yamazaki T, et al. Subfoveal choroidal thickness in typical age-related macular degeneration and polypoidal choroidal vasculopathy. Graefes Arch Clin Exp Ophthalmol. 2011; 249:1123–8. [PubMed: 21274555]

21. Zhang L, Lee K, Niemeijer M, et al. Automated segmentation of the choroid from clinical SD-OCT. Invest Ophthalmol Vis Sci. 2012; 53:7510–9. [PubMed: 23060139]

22. Sohrab M, Wu K, Fawzi AA. A pilot study of morphometric analysis of choroidal vasculature in vivo, using en face optical coherence tomography. PLoS One [serial online]. 2012; 7:e48631. Available at: http://www.plosone.org/article/info%3Adoi%2F10.1371%2Fjournal.pone.0048631.

23. Manjunath V, Taha M, Fujimoto JG, Duker JS. Choroidal thickness in normal eyes measured using Cirrus HD optical coherence tomography. Am J Ophthalmol. 2010; 150:325–9. [PubMed: 20591395]

24. Margolis R, Spaide RF. A pilot study of enhanced depth imaging optical coherence tomography of the choroid in normal eyes. Am J Ophthalmol. 2009; 147:811–5. [PubMed: 19232559]

25. Anger EM, Unterhuber A, Hermann B, et al. Ultrahigh resolution optical coherence tomography of the monkey fovea. Identification of retinal sublayers by correlation with semithin histology sections. Exp Eye Res. 2004; 78:1117–25. [PubMed: 15109918]

26. Unterhuber A, Povazay B, Hermann B, et al. In vivo retinal optical coherence tomography at 1040 nm - enhanced penetration into the choroid. Opt Express [serial online]. 2005; 13:3252–8. Available at: http://www.opticsinfobase.org/oe/abstract.cfm?uri=oe-13-9-3252.

27. Povazay B, Bizheva K, Hermann B, et al. Enhanced visualization of choroidal vessels using ultrahigh resolution ophthalmic OCT at 1050 nm. Opt Express [serial online]. 2003; 11:1980–6. Available at: http://www.opticsinfobase.org/oe/abstract.cfm?uri=oe-11-17-1980.

28. Izatt JA, Kulkarni MD, Yazdanfar S, et al. In vivo bidirectional color Doppler flow imaging of picoliter blood volumes using optical coherence tomography. Opt Lett. 1997; 22:1439–41. [PubMed: 18188263]

29. Leitgeb R, Schmetterer L, Drexler W, et al. Real-time assessment of retinal blood flow with ultrafast acquisition by color Doppler Fourier domain optical coherence tomography. Opt Express [serial online]. 2003; 11:3116–21. Available at: http://www.opticsinfobase.org/oe/abstract.cfm?uri=oe-11-23-3116.

30. White B, Pierce M, Nassif N, et al. In vivo dynamic human retinal blood flow imaging using ultra-high-speed spectral domain optical coherence tomography. Opt Express [serial online]. 2003; 11:3490–7. Available at: http://www.opticsinfobase.org/oe/abstract.cfm?uri=oe-11-25-3490.

31. Wang Y, Fawzi AA, Varma R, et al. Pilot study of optical coherence tomography measurement of retinal blood flow in retinal and optic nerve diseases. Invest Ophthalmol Vis Sci. 2011; 52:840–5. [PubMed: 21051715]

32. Srinivasan VJ, Adler DC, Chen Y, et al. Ultrahigh-speed optical coherence tomography for three-dimensional and en face imaging of the retina and optic nerve head. Invest Ophthalmol Vis Sci. 2008; 49:5103–10. [PubMed: 18658089]

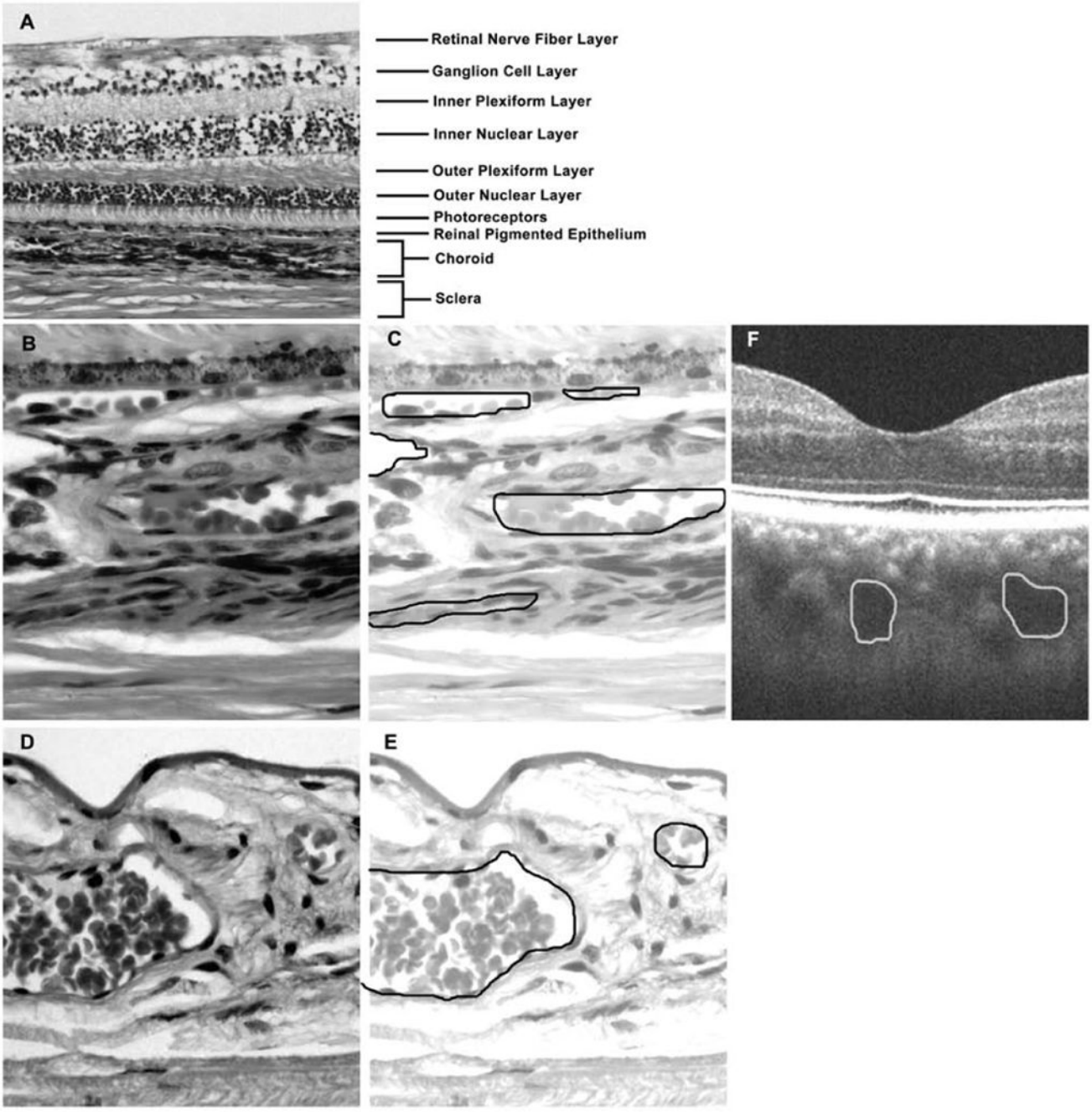

Figure 1.

Choroidal histology of healthy eye and that affected with age-related macular degeneration (AMD). The histology of the healthy eye is compared with spectral domain optical coherence tomography (SD-OCT) image. (A) Hematoxylin and eosin (H&E) stained section of peri-macular full-thickness retina and choroid of a healthy donor eye (4x). Black lines denote retinal layers as identified. (B) High magnification (60x) H&E stained section of peri-macular choroid in a healthy donor eye. (C) Schematic demonstrating (black) outlines of choroidal vessels in the choriocapillaris layer (small vessels), medium choroidal vessel layer (Sattler's layer) (medium-sized vessels) and large choroidal vessel layer (Haller's layer) (large-sized vessels). (D) High magnification (60x) H&E stained section of peri-

macular choroid from a donor eye with age-related macular degeneration (E) Schematic demonstrating (black) outlines of a medium choroidal vessel layer (Sattler's layer) (medium-sized vessels) and large choroidal vessel layer (Haller's layer) (large-sized vessels). Note the absence of choriocapillaris in this case. (F) SD-OCT image of the fovea of a healthy subject (white) lines outline large choroidal vessels.

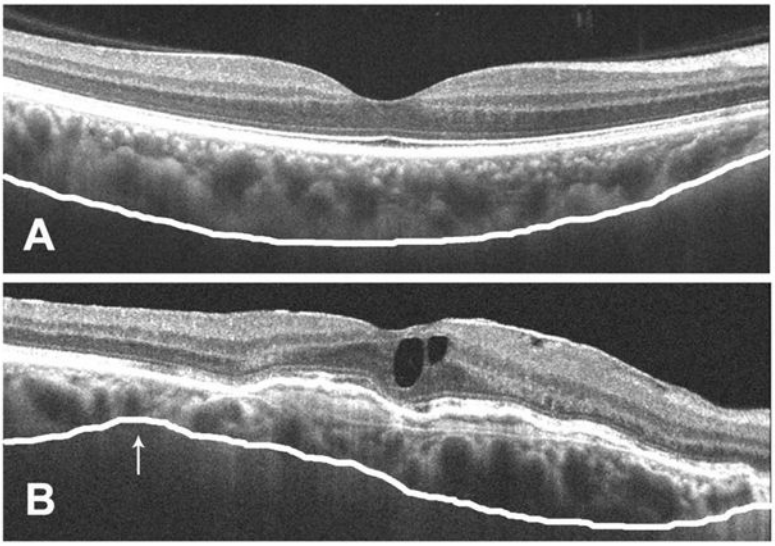

Figure 2.
Choroidal imaging with spectral-domain optical coherence tomography (SD-OCT) of a healthy eye and that with age-related macular degeneration (AMD). (A) SD-OCT image of a healthy subject. Note the “bowl” shape to the border of the choroid and sclera (white line), even distribution of large choroidal vessels in the nasal-temporal plane, even continuum of choroidal vessel size (large-small from outer choroid to inner choroid). (B) SD-OCT image of a patient with AMD. Note the irregular “S” shaped border of the choroid and sclera (white line) with focal thinning of the choroid (white arrow) and the thickest point of the choroid not below the fovea. Also note the close proximity of large choroidal vessels to Bruch’s membrane/retinal pigment epithelium.

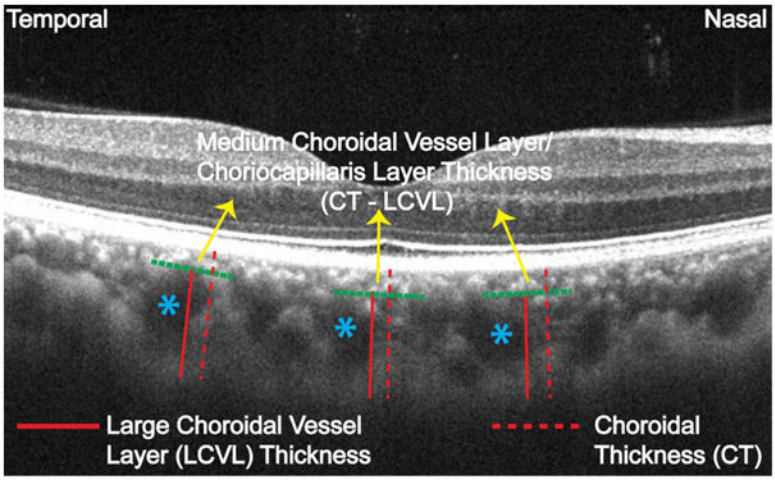

Figure 3.

Illustration of the method used to analyze the choroidal vasculature on a spectral domain optical coherence tomography (SD-OCT) image of a healthy eye. Blue asterisks represent the large choroidal vessels seen in the closest proximity to the three locations of vasculature analysis, that is, at the fovea, 750μm temporal to the fovea and 750μm nasal to the fovea, and closest to the choroidal- scleral border, which were selected for the large choroidal vessel layer measurements. Large choroidal vessel layer thickness was measured from the inner border of the choroid-scleral junction to the innermost point of the selected large choroidal vessel at each location. All measurements were performed using the Cirrus linear measurement tool.

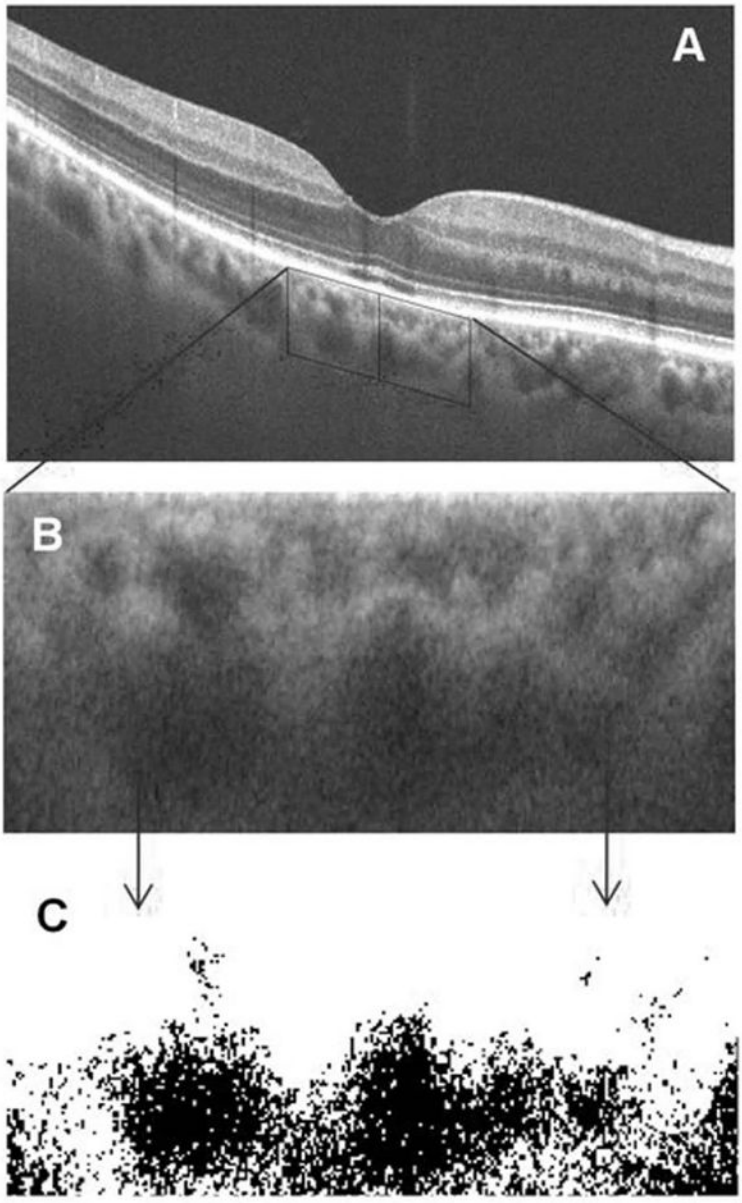

Figure 4.
Illustration of the method used for light dark ratio analysis to calculate the ratio of the region of choroidal stroma to the region of choroidal vessel lumen. (A) Spectral-domain optical coherence tomography image (SD-OCT) of a healthy eye. Black box represents the selection of the sub-foveal choroidal region of interest (ROI). (B) Magnified section of ROI. (C) ROI after software analysis. White area (bright pixels) represents the choroidal stroma and black area (black pixels) represents choroidal vessel lumen.

Table 1

Morphological features of the choroid in healthy eyes. n represents the total number of healthy eyes analyzed.

CHOROIDAL MORPHOLOGY FEATURE	% of Healthy Eyes with Choroidal Feature
1. “Bowl” shape to the border of the choroid and sclera (1 point of inflection)	100%
2. Reflectance between large choroidal vessels hypo-intense and heterogenous	100%
3. Even distribution of the large choroidal vessels in the nasal-temporal plane	98.8%
4. Even continuum of choroidal vessel size (large-small from outer choroid to inner choroid	97.6%
5. Clarity of the choroid-scleral border	92.8%
6. Thickest point of choroid beneath the fovea	88.0%
7. Scleral vessel penetration into the choroid	9.5%
8. Focal thinning of the choroid	0.0%

Table 2

Analysis of the choroidal vasculature in healthy eyes. p values represent the results of Pearson correlation

CHOROIDAL VASCULATURE ANALYSIS				
	750 μm TEMPORAL	**SUB-FOVEAL**	**750 μm NASAL**	**INTER-OBSERVER CORRELATION**
Total Choroidal Thickness (CT) (μm)	255.0 ± 75.7	256.8 ± 75.8	243.2 ± 69.3	0.98; p<0.0001
Large Choroidal Vessel Layer (LCVL) Thickness (μm)	203.7 ± 60.3	204.3 ± 65.9	198.6 ± 62.5	0.91; p<0.0001
Medium Choroidal Vessel Layer/Choriocapillaris Layer Thickness (μm)	51.7 ± 23.1	52.9 ± 20.6	44.7 ± 19.7	----
Ratio of LCVL to CT	0.8 ± 0.05	0.7 ± 0.06	0.8 ± 0.06	----